Biochemical and Structural Characterization of the Interaction of Memapsin 2 (β-Secretase) Cytosolic Domain with the VHS Domain of GGA Proteins†

Xiangyuan He,‡ Guangyu Zhu,§ Gerald Koelsch,‡,|| Karla K. Rodgers,⊥ Xuejun C. Zhang,§ and Jordan Tang*,‡,⊥

Protein Studies Program and Crystallography Program, Oklahoma Medical Research Foundation, 825 Northeast 13th Street, Oklahoma City, Oklahoma 73104, and Department of Biochemistry and Molecular Biology, Oklahoma University Health Sciences Center, Oklahoma City, Oklahoma 73104

Received July 9, 2003; Revised Manuscript Received August 26, 2003

ABSTRACT: Memapsin 2 (β-secretase) is a membrane-associated aspartic protease that initiates the hydrolysis of β-amyloid precursor protein (APP) leading to the production of amyloid-β and the onset of Alzheimer's disease (AD). Both memapsin 2 and APP are transported from the cell surface to endosomes where APP hydrolysis takes place. Thus, the intracellular transport mechanism of memapsin 2 is important for understanding the pathogenesis of AD. We have previously shown that the cytosolic domain of memapsin 2 contains an acid-cluster-dileucine (ACDL) motif that binds the VHS domain of GGA proteins (He et al. (2002) *FEBS Lett. 524*, 183−187). This mechanism is the presumed recognition step for the vesicular packaging of memapsin 2 for its transport to endosomes. The phosphorylation of a serine residue within the ACDL motif has been reported to regulate the recycling of memapsin 2 from early endosomes back to the cell surface. Here, we report a study on the memapsin 2/VHS domain interaction. Using isothermal titration calorimetry, the dissociation constant, K_d, values are 4.0×10^{-4}, 4.1×10^{-4}, and 3.1×10^{-4} M for VHS domains from GGA1, GGA2, and GGA3, respectively. With the serine residue replaced by phosphoserine, the K_d decreased about 10-, 4-, and 14-fold for the same three VHS domains. A crystal structure of the complex between memapsin 2 phosphoserine peptide and GGA1 VHS was solved at 2.6 Å resolution. The side chain of the phosphoserine group does not interact with the VHS domain but forms an ionic interaction with the side chain of the C-terminal lysine of the ligand peptide. Energy calculation of the binding of native and phosphorylated peptides to VHS domains suggests that this intrapeptide ionic bond in solution may reduce the change in binding entropy and thus increase binding affinity.

Memapsin 2 (*1*), also called BACE (*2*), ASP-2 (*3, 4*), and β-secretase, is a protease that initiates the cleavage of the β-amyloid precursor protein (APP).[1] Proteolysis by memapsin 2 and another protease, γ-secretase, produces a 40- or 42-residue peptide called amyloid-β (Aβ). An excessive level of brain Aβ leads ultimately to the death of neurons and the progression of Alzheimer's disease (*5*). To understand the involvement of memapsin 2 in the pathogenesis of AD, information on the cellular transport and activity of this protease is of great importance.

Memapsin 2 is a type I membrane protein with a single transmembrane segment linking a luminal catalytic unit, homologous to other mammalian aspartic proteases (*6*), to a C-terminal cytosolic tail (C-tail) of 21 residues. The newly synthesized pro-memapsin 2 is processed to mature protease by furin during transit through the secretory pathway to the cell surface (*7*−*10*). Memapsin 2 is active in an acidic medium up to pH 5 (*1, 2, 11*); thus, it is out of the pH range of its activity at the cell surface. Both APP and memapsin 2 at the cell surface are internalized to endosomes, the main site for APP cleavage by memapsin 2 and the production of Aβ. The memapsin 2 protease is then recycled to the cell surface (*10, 12*). The structural signal required for the endocytosis of memapsin 2 was found to be a commonly used Leu−Leu motif present in the C-tail (*10, 13*). More recently, an aspartic acid and two leucine residues within a DISLL sequence in the memapsin 2 C-tail were shown to mediate the binding of memapsin 2 to the VHS (Vps-27, Hrs, and STAM) domains of GGA (Golgi-localized γ-ear-containing ARF binding) proteins (*14*). This memapsin 2 motif appears to be a form of the acidic-cluster-dileucine (ACDL) sorting signal DXXLL (X denotes a nonconserved residue) found in the cytosolic tails of mannose-6-phosphate receptors (MPRs; refs *15*−*17*) and other lysosomal membrane proteins (*17, 18*). The binding of ACDL in these proteins to GGA VHS is responsible for the recruitment of these receptors to the coated vesicles on the trans-Golgi membrane for transporting to endosomes and ultimately to lysosomes (*15*−*18*). In the case of MPRs, this interaction

† This work was supported in part by NIH Grant AG-18933 and Alzheimer's Association Pioneer Award to J.T. and NIH Grant HL60626 to X.C.Z.

* To whom correspondence should be addressed. Tel: (405) 271-7291. Fax: (405) 271-7249. E-mail: Jordan-tang@omrf.ouhsc.edu.

‡ Protein Studies Program, Oklahoma Medical Research Foundation.

§ Crystallography Research Program, Oklahoma Medical Research Foundation.

|| Current address: Zapaq Inc., 825 NE 13th Street, Oklahoma City, OK 73104.

⊥ University of Oklahoma Health Sciences Center.

[1] Abbreviations: Aβ, amyloid-β; ACDL, acidic-cluster-dileucine; APP, β-amyloid precursor protein; CI-MPR, cation-independent MPR; GGA, Golgi-localized γ-year-containing ARF binding; MPR, mannose-6-phosphate receptor; VHS, Vps-27, Hrs, and STAM.

10.1021/bi035199h CCC: $25.00
Published on Web 10/01/2003

Table 1: Equilibrium Dissociation Constants of VHS Domain Binding to Memapsin 2 Cytosolic Peptides

Source of Cytosolic peptide	Peptide Name	Sequence [a]	Source of VHS	K_d ($\times 10^{-5}$ M)
CI-MPR	CI-MPR-17	CKLVSFHDDS**D**E**D**L**L**HI	GGA2	1.07 ± 0.06
Memapsin 2	M2-17	CLRQQHDDFAD**D**IS**LL**K	GGA2	28.7 ± 3.2
Memapsin 2	M2-17(IS/AA)	CLRQQHDDFAD***DAA***L**L**K	GGA2	18.4 ± 2.1
Memapsin 2	M2-17(D495A)	CLRQQHDDFA***A***D**D**IS**LL**K	GGA2	30.3 ± 3.2
Memapsin 2	M2-17(D496A)	CLRQQHDDFAD***A***I**D**S**LL**K	GGA2	>100
Memapsin 2	M2-17(L499A)	CLRQQHDDFAD**D**IS***A***L**L**K	GGA2	>100
Memapsin 2	M2-17(L500A)	CLRQQHDDFAD**D**IS**L*****A***K	GGA2	>100
Memapsin 2	M2-8	A**D**D**D**IS**LL**K	GGA1	39.9 ± 4.1
Memapsin 2	M2-8($S498S_P$)	A**D**D**D**I***S*****$_p$**L**L**K	GGA1	4.0 ± 0.5
Memapsin 2	M2-8	A**D**D**D**IS**LL**K	GGA2	41.2 ± 5.2
Memapsin 2	M2-8($S498S_P$)	A**D**D**D**I***S*****$_p$**L**L**K	GGA2	10.1 ± 0.4
Memapsin 2	M2-8	A**D**D**D**IS**LL**K	GGA3	30.7 ± 2.5
Memapsin 2	M2-8($S498S_P$)	A**D**D**D**I***S*****$_p$**L**L**K	GGA3	2.2 ± 0.3

[a] Sequences are shown in single letter amino acid code. The essential residues (Asp^{496}, Leu^{499}, and Leu^{500}) for VHS binding are shown in boldface for orientation. The substituted residues are shown in italics, and phosphoserine is shown as S_P.

serves as the basis for targeting newly synthesized lysosomal enzymes. Therefore, GGA binding of the DISLL motif of memapsin 2 suggests that it is involved in the endocytosis and/or Golgi to endosome transport of memapsin 2 (*14*).

Phosphorylation near the ACDL motif may enhance its interaction with GGAs. In cation-independent MPR (CI-MPR), the phosphorylation, which occurs in vivo (*19*−*21*), takes place at the serine in the sequence of SDEDLL (*22*). The phosphorylated CI-MPR peptide produces a moderate increase in affinity toward GGA proteins (i.e., the K_d is lowered by 3−4-fold for CI-MPR (*22*)). The phosphorylation of the DISLL motif of memapsin 2, however, is at the serine residue within the motif. The mutation of this serine to an alanine altered the intracellular distribution of memapsin 2, suggesting that the phosphorylation plays a role in the transport of this protease (*12*, *13*). The difference in position and consequences due to the phosphorylation of these two ACDL motifs argues that the phosphorylation regulates the trafficking of these proteins. In addition to the VHS domain, GGA proteins contain three other domains that interact with other proteins participating in vesicular transport, such as clathrin, AP-1, and Rabaptin5 proteins (*23*, *24*). Crystal structures for the complex of unphosphorylated (*25*, *26*) and phosphorylated (*22*) ACDL containing peptides from CI-MPR with VHS domains of GGA1 and GGA3 have been determined. These structures confirm the important recognition roles of aspartic acid, dileucine, and phosphoserine in the ACDL motif. Molecular modeling for the binding of a DISLL-containing memapsin 2 peptide to the crystal structure of VHS from GGA2 revealed a very similar interaction to that of CI-MPR/VHS (*27*). To further understand the interaction of memapsin 2 ACDL motif with VHS, we determined the binding affinity of both phosphorylated and nonphosphorylated peptides with VHS domains from all three GGAs and the crystal structure of a phosphorylated peptide complexed with GGA1 VHS. Our results suggest that all three GGAs interact with the memapsin 2 C-tail in a similar manner and that the phosphorylation enhances the interaction.

MATERIALS AND METHODS

cDNA Cloning and Protein Expression. The preparation of the fusion protein of glutathione-*S*-transferase(GST) and VHS/GGA1 or VHS/GGA2 has previously been described (*14*). For constructing VHS/GGA3 fusion, a fragment of GGA3 cDNA (GenBank accession number AF219138), corresponding to residues 1−157, was amplified from a human placenta long-insert cDNA library (Clontech), and the construction of its GST fusion protein, expression, and purification were the same as previously described (*14*). For crystallography and isothermal titration studies, recombinant GST-VHS/GGA1 was first purified through a glutathione-sepharose 4B affinity column, and then the GST moiety was cleaved off with biotinilated thrombin (Novagen, Darmstadt, Germany). The digested sample was mixed with glutathione-sepharose and centrifuged. The supernatant containing free VHS/GGA1 was further purified with Resource Q ion-exchange chromatography (Amersham-Pharmacia), dialyzed against a buffer of 1 mM Tris-HCl (pH 8.4) and 0.1% (v/v) β-mercaptoethanol, concentrated to 14 mg/mL (~0.8 μM), and stored at −80 °C before use.

Isothermal Titration Calorimetry. The nomenclature and sequences of the peptides derived from the cytosolic domain of memapsin 2 are listed in Table 1. The design and synthesis of these peptides are as described before (*14*). The phos-

phopeptide ADDIS$_P$LLK, where S$_P$ represents a phosphoserine, was synthesized at ResGenetics (Huntsville, AL). The purified GST-VHS fusion proteins from three GGAs were dialyzed into phosphate-buffered saline (PBS), pH 7.4, with 1 mM dithiothreitol (DTT), and their concentrations were adjusted to 50 μM. The ligand peptides were dissolved in the same buffer to 1 mM. Isothermal calorimetric titrations were performed in a VP-ITC microcalorimeter (MicroCal Inc., Northampton, MA) at 30 °C. The peptide solutions were injected into the VHS solution (1.4 mL) or a blank buffer (i.e., without VHS) that served as a blank run to be subtracted from the experimental data. The equilibrium dissociation constant (K_d), entropy, and enthalpy were determined using the calorimetric analysis program ORIGIN (supplied by Microcal, Inc.). The experimentally determined stoichiometry for VHS of all three GGAs toward the peptide ligands was essentially 1:1 for all experiments.

Cell Culture and Antibodies. The construct of hemaglutinin (HA)-tagged GGA1 was kindly provided by Dr. K. Nakayama (Kanazawa University, Japan). The constructs of GGA2-V5 and GGA3-V5 were amplified by PCR and inserted into plasmid pcDNA6.1 (Invitrogen). They were transiently transfected into HEK 293 cells using transfection reagent LipofectAMINE 2000 (Invitrogen). Cells were grown in Dulbecco's Modified Eagle's medium (DMEM) containing 10% fetal bovine serum, 100 U/mL penicillin, and 100 μg/mL streptomycin (GibcoBRL). Cells were collected and lysed on ice in PBS with 1% Nonidet P-40. Monoclonal mouse antibodies to hemagglutinin (HA) were purchased from Sigma. Monoclonal mouse antibodies to the V5 tag were purchased from Invitrogen.

Pull-Down Experiments. The peptides derived from memapsin 2 (M2-17, see Table 1 for sequence) and CI-MPR (CI-MPR-17) were covalently linked by their thiol groups to Sulfolink Coupling Gel (Pierce) using the procedure recommended by the manufacturer. Cell lysates were prepared from HEK-293 cells transfected separately with HA-GGA1 and GGA2-V5 and GGA3-V5 expression vectors. Cell lysates, each containing 200 μg of protein, were incubated with 100 μL of gel bearing immobilized peptide in 1.5 mL of PBS at room temperature for 2 h. The gel beads were pelleted by centrifugation at 750*g* for 1 min and washed three times with PBS. The proteins on the gel beads were eluted by sodium dodecyl sulfate(SDS)-containing sample buffer and subjected to SDS−PAGE (10% gel) electrophoresis. GGA bands were identified by Western blot using monoclonal anti-HA or anti-V5 antibody. The negative control was the same as previously described (*14*).

Crystallization. The initial crystallization condition was found with commercial crystallization screen kits (Hampton Research, Laguna Niguel, CA). Crystals used for data collection were grown at 20 °C from hanging drops under the following conditions. Freshly thawed protein solution was mixed 4:1 (v/v) with a solution of 20 mM peptide ADDIS$_P$-LLK (S$_P$, phosphoserine; see Figure 1). This solution was further mixed 2:1 (v/v) with the precipitant solution consisting of 30% (w/v) poly(ethylene glycol) MW 3350, 0.2 M ammonium sulfate, 0.1 M sodium cacodylate (pH 6.4), and 0.1% (v/v) β-mercaptoethanol. Crystals appeared in 1 day after microseeding and grew to full size (0.05 × 0.3 × 0.3 mm) in about one week. The same reservoir solution supplemented with 10% (v/v) glycerol was used as a cryo-

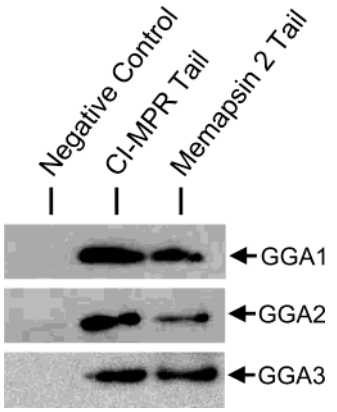

FIGURE 1: SDS−PAGE electrophoresis pattern of the pull-down of GGA proteins by memapsin 2 cytosolic peptide MP-8 immobilized on gel beads (see Table 1 for sequence). Full-length GGAs were separately expressed in HEK293 cells. The cell lysates were incubated separately with a gel-linked peptide (or a cysteine-blocked gel for negative controls), and the washed gel samples were subjected to SDS−PAGE and Western blotting for visualization of bound GGAs. CI-MPR peptide (CI-MPR-17, Table 1) was used as a positive control.

solution to soak the crystals before being cooled in a 100 K nitrogen gas stream for data collection.

Data Collection, Structure Determination, and Refinement. A complete set of X-ray diffraction data was collected at 2.6 Å resolution from a MAR345 image-plate (Mar Research Inc. Norderstedt, Germany) and Rigaku X-ray generator (Molecular Structure Co., Woodlands, TX) equipped with an Osmic mirror system (Osmic Inc., Troy, MI). Data were processed with the program suite *HKL* (*28*). The crystal form belongs to the space group $P2_12_12$. One asymmetric unit contains four VHS molecules with 51% solvent content (*29*). The solution for the crystal structure was determined using molecular replacement methods with the program *AMoRe* (*30*) and the crystal structure of VHS/GGA1 (PDB code 1JWF, ref *26*) as a template. Model building was carried out with the program *Turbo-Frodo* (*31*). The VHS/GGA1 crystal structure was refined using simulated annealing with the program suite *CNS* (*32*) to a 0.235 *R*-factor with excellent geometry (Table 2).

RESULTS AND DISCUSSION

Binding of Memapsin 2 Cytosolic Peptides to VHS Domains of GGA Proteins. The binding of a memapsin 2 peptide to the VHS domain of GGA1 and GGA3 had previously been shown (*14*). In Figure 1, we show that all three GGAs from cell lysates were pulled down by gel-immobilized memapsin 2 C-tail peptide. As in GGA1 and GGA3 (*14*), the CI-MPR peptide was more efficient in pulling down GGA2 than was the memapsin 2 peptide.

We then determined, by using isothermal titration calorimetry, the dissociation constants for the binding of memapsin 2 cytosolic peptides (Table 1) to VHS domains of the three GGAs. The K_d value for the binding of a 17-residue memapsin 2 peptide, M2-17, to GGA2 VHS (2.87×10^{-4} M) is 27 times higher than that for the corresponding peptide from CI-MPR (1.07×10^{-5} M). The latter value agrees well with that reported for the binding of CI-MPR cytosolic peptide to GGA1 (0.79×10^{-5} M) and GGA3 (1.09×10^{-5} M) (*22*). The lower K_d for the CI-MPR peptide than that for

Table 2: Crystallography Data Collection and Refinement Statistics

Data Statistics	
space group	$P2_12_12$
unit cell (Å)	
a	70.1
b	95.4
c	108.0
resolution (Å)	40 (2.69)[a] − 2.60
R_{merge} (%)	7.4 (47.7)[a]
no. of reflections	22869 (2229)[a]
completeness (%)	99.5 (98.9)[a]
redundancy	6.9
$I/\sigma(I)$	25.8 (3.6)[a]
Refinement Statistics	
$R_{working}$ (%)/no. of reflections [b]	23.6/21148
R_{free} (%)/no. of reflections[b]	28.8/858
no. of non-hydrogen atoms	
protein	4511
ligand peptide	232
solvent	37
rms deviation from ideal values	
bond length (Å)	0.011
bond angle (deg)	1.20
average *B*-factor (Å^2)	
protein	49 (47)[c]
ligand peptide	67
solvent	37

[a] Numbers in parentheses are the corresponding numbers for the highest resolution shell. [b] Reflections of $|F_{obs}| > 0.0$. [c] The number in parentheses is the *B*-factor estimated from the Wilson plot.

the memapsin 2 peptide is consistent with the observation that the former is more efficient in pull-down experiments (Figure 1 and ref *14*). We also confirmed the importance of the aspartic acid and dileucine in the motif of DISLL for binding to VHS. The replacement of the sequence IS in the motif (peptide M2-17(IS/AA)) or of the aspartic acid preceding the motif (peptide M2-17(D495A) by alanines did not significantly change the K_d value from that of the native peptide (Table 1). Single replacement of aspartic acid (peptide M2-17(D496A) or either leucine residues (peptides M2-17(L499A) and M2-17(L500A)), however, dramatically increased the K_d for VHS of GGA2 to above 10^{-3} M; thus, these values could not be accurately determined. We have also observed a similar high value of K_d for these last three peptides for binding to VHS from GGA1 and GGA2 (results not shown). We also found that the K_d value (42.1×10^{-5} M) for the binding of the C-terminal eight residues of memapsin 2 (peptide M2-8) to VHS/GGA2 is close to that for the longer peptide M2-17 (Table 1). This observation confirmed that the interaction of memapsin 2 C-tail rests essentially in the DISLL motif.

The effect of phosphorylation of memapsin 2 Ser^{498} in the DISLL motif on VHS binding was studied. Phosphorylation of the octapeptide, M2-8, decreased the K_d by 10-fold for GGA1 (from 4×10^{-4} to 4×10^{-5} M), 4-fold for GGA2 (from 4×10^{-4} to 1×10^{-4} M), and 14-fold for GGA3 (from 3.1×10^{-4} to 2.2×10^{-5} M) (Table 1). As a comparison, the phosphorylation of the CI-MPR cytosolic peptide decreases the K_d of GGA1 and GGA2 binding by 4- and 3-fold, respectively (*22*). Walter et al. (*12*) have reported that phospho-Ser^{498} does not significantly alter the endocytic pathway of memapsin 2, rather it plays a role for recycling of this protease from early endosome via late endosome and/or TGN to the cell surface. The current observation that the phosphorylation increased binding intensity to all three GGAs suggests that GGA proteins may be involved in memapsin 2 recycling.

Crystal Structure of Memapsin 2 Phosphoserine Peptide Binding to VHS/GGA1. The crystal structure of the human GGA1 VHS domain (residues 2−157) complexed with the memapsin 2 phosphoserine peptide M2-8(S498S$_P$) (Table 2) was determined at 2.6 Å resolution. The crystal was in a $P2_12_12$ space group with four VHS molecules in an asymmetric unit, each bound to a ligand peptide. In the final refined structure, five to six residues at the N-terminus and up to 12 residues at the C-terminus of GGA1 VHS did not have interpretable electron density. However, these residues are not directly involved in ligand binding. The statistics of data collection and refinement are shown in Table 2. Coordinates of this VHS structure have been deposited to the Protein Databank (PDB code 1PY1).

Structures of the four VHS/GGA1 molecules in the asymmetric unit were essentially identical to each other and were very similar to those previously reported GGA VHS domains (*25*−*27*). Each protein molecule contains a right-handed superhelix of eight helices ($\alpha1-\alpha8$) divided into two layers. The C_α atom root-mean-square deviation (rmsd) between GGA1 VHS molecules ranged between 0.29 and 0.50 Å (residues 8−145). The four VHS molecules in an asymmetric unit formed two identical, symmetric dimers. This appears to be the prevalent form of VHS domain packing, as similar dimers have been observed (*27*) from crystals derived under different crystallization conditions.

Molecular Interactions of Memapsin 2 Phosphoserine Peptide with GGA1 VHS. The eight-residue peptide cocrystallized with the VHS domain consists of a sequence of ADDIS$_P$LLK, which contains the VHS binding motif DISLL and where the phosphoserine (S$_P$) is at the fifth position. In all four VHS−ligand complexes of the asymmetric unit, the phosphopeptide binds to the previously reported ACDL ligand binding site (Figure 2A) (i.e., between helices $\alpha6$ (residues 89−98), $\alpha8$ (residues 130−142), and the loop $L_{6,7}$ (residues 98−107) (*25*, *26*)). The N-terminal alanine residue is mobile in all four structures. The overall binding mode and the specific interactions of three essential residues were practically the same as those of MPR peptides binding to GGA1 (*26*) and GGA3 (*22*, *25*). Briefly, the essential aspartic acid (D3 in Figure 2) interacts with three basic groups of GGA1 VHS, Lys^{87}, Arg^{89}, and Lys^{131}. One of the essential Leu residues (L6 in Figure 2) is interacting with Phe^{88}, Met^{138}, and Ile^{95}, while the other (L7) interacts with Lys^{96} and Tyr^{102}. For the non-motif residues, the free carboxyl at the C-terminal lysine (K8) interacts with three VHS residues, Lys^{101}, Tyr^{102}, and Gln^{142}. From sequence alignment, the CI-MPR cytoplasmic tail is one residue longer at the C-terminus than memapsin 2 (Table 1, see also the overlay of two peptide ligands in Figure 2B). The peptide carbonyl in CI-MPR corresponding to the memapsin 2 C-terminal carboxyl does interact with Lys^{101} and Tyr^{102} and somewhat weakly with Gln^{142}. In the current structure, GGA1 VHS residues involved in ligand binding are conserved as previously pointed out by Shiba et al. (*26*). Memapsin 2 peptide side chains aspartic acid (D2) and isoleucine (I4) are devoid of significant interaction with VHS residues. This presumably contributes to the difference between the binding intensity of memapsin 2 and CI-MPR peptides to GGA1 VHS (see next). In the

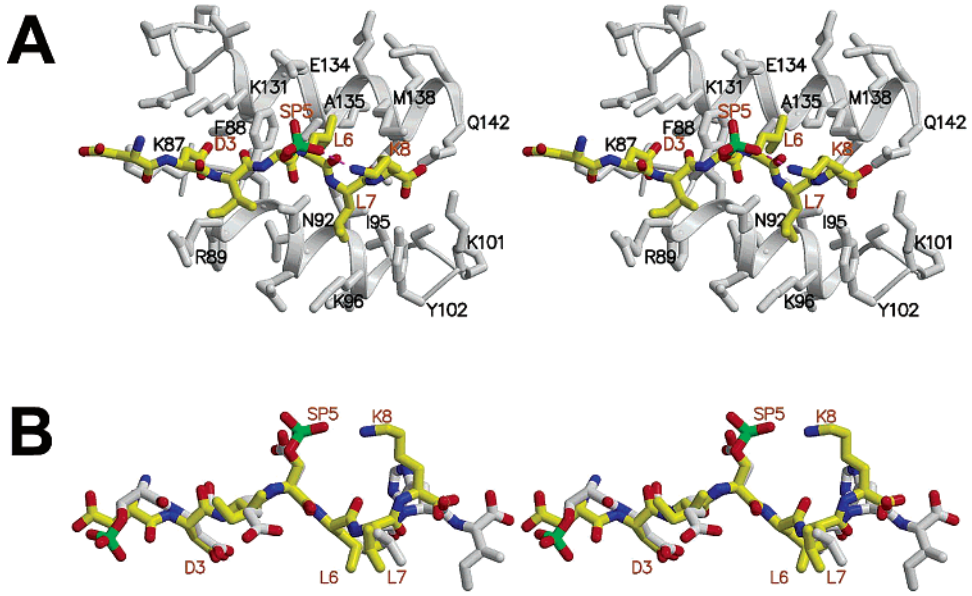

FIGURE 2: Stereoview of phosphorylated memapsin 2 cytosolic peptide MP-7(S498S$_P$). (A) Crystal structure of MP-7(S49S$_P$) interacting with the ligand binding site of GGA1 VHS domain (gray). The atoms in the peptide ligand are colored as follows: carbon, yellow; oxygen, red; nitrogen, blue; and phosphate, turquoise. The VHS residues are labeled in black and the ligand residues in light brown. The hypothesized ionic interaction between phosphoserine SP5 and K8 are shown in a dark broken line. (B) Superposition of peptide MP-7(S298S$_P$) (gray) with phosphorylated CI-MPR peptide (color code as in panel A) from a complex with GGA3 VHS (PDB file 1LF8), guided by an overlaying of the corresponding VHS domains. Only the MP-7 residues are marked.

current structure, the side chain of phosphoserine (SP5) protrudes into the solvent with a clearly defined electron density, even though its average *B*-factor was relatively high (75 Å^2). The side chain of the C-terminal lysine residue was observed pointing to the phosphate group of the phosphoserine (see Figure 2).

Comparing the Binding of Memapsin 2 and CI-MPR Cytosolic Peptides to VHS. GGA1 VHS binds CI-MPR peptide, CI-MPR-17, with about a 27-fold lower K_d value than the corresponding memapsin 2 peptide, M2-17 (Table 1), despite the close similarity in the bound conformation of the two ligands (Figure 2B). The structural difference that may account for the difference in binding intensity was sought by comparing crystal structures of GGA1 VHS complexed with M2-8(S498S$_P$) (current structure) and CI-MPR peptide (*26*). The interactions of three essential residues to VHS are almost identical in these two structures. However, differences were seen in the binding of nonessential residues. The C-terminal Ile in CI-MPR, which is surrounded by Ile^{94}, Ser^{99}, Met^{138}, Gln^{142}, and Ile^{144} in GGA1 VHS (PDB code 1JWG), is absent in memapsin 2. In addition, while the glutamic acid that follows the essential aspartic in CI-MPR has an ionic interaction with Arg^{89} of GGA1 VHS, the corresponding isoleucine in the memapsin 2 peptide is devoid of significant interaction. These differences in interaction appear sufficient to produce a 27-fold difference in K_d values. The difference in binding intensity between GGAs and various ACDL motifs has not been previously reported, and its biological consequence is not clear. The difference seems large enough to provide sorting specificity among intracellular trafficking pathways.

Phosphorylation of the serine residue in the memapsin 2 peptide produced an enhanced binding to VHS of all three GGAs. The K_d values are 10, 4, and 14 times lower after the phosphorylation of the M2-8 peptide for GGA1, GGA2, and GGA3, respectively (Table 1). The binding intensity of the phosphorylated memapsin 2 peptide approximates that of CI-MPR, especially for GGA3. The phosphorylation of the memapsin 2 C-tail is known to play a role in the recycling of this protease from the early endosomes back to the cell surface (*12*). The increased VHS binding of phosphorylated memapsin 2 suggests that GGAs may participate in this recycling process. In the case of CI-MPR, the phosphorylation of the serine (10th residue in peptide CI-MPR-17, see Table 1) resulted in new ionic interactions of the phosphate group with two basic side chains, Lys^{86} and Arg^{88}, of GGA3 VHS (*22*). In the memapsin 2 peptide, the residue corresponding to the CI-MPR phosphoserine is an aspartic acid (second residue in the M2-8 peptide), which could form a similar ionic interaction but is nevertheless mobile (i.e., of higher *B*-factors) in the crystal structure. The new phosphate group in the memapsin 2 peptide is actually in an ionic interaction with the C-terminal lysine in the ligand itself (Figure 2). Since it is the only interaction in the memapsin 2 peptide/VHS structure not seen in the CI-MPR/VHS structure, this new interaction seems likely to comprise the structural basis for the significant increase in binding intensity with VHS domains after the phosphorylation of the memapsin 2 peptide (Table 1). A plausible explanation is summarized in Figure 3. The charge distribution of the memapsin 2 C-terminal peptide is such that it prefers an extended structure in solution (Figure 3, upper left). The phosphorylation of the serine residue (Figure 3, lower left) changes the charge distribution and results in a new preferred conformation (Figure 3, upper right) that permits the interaction of the new phosphate group with the C-terminal lysine and avoids two negatively charged aspartyl groups in close vicinity. In the preferred conformation, all three essential groups, an aspartic acid and two leucines, are located on the same side (Figure 3, lower right and Figure 2B) for efficient binding to the VHS domain. Such a mechanism is energetically favorable since it minimizes the entropy loss resulting from peptide

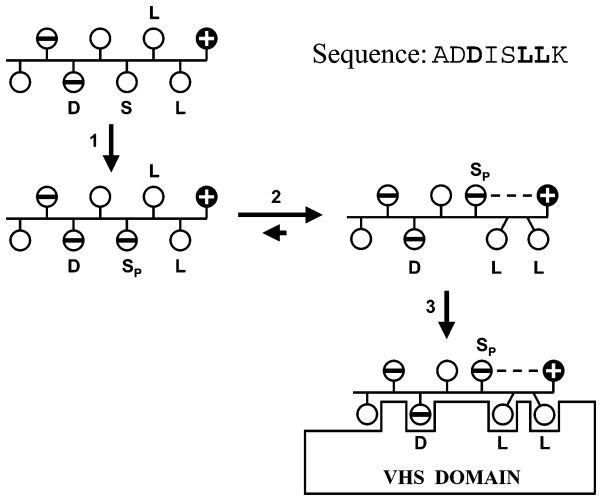

FIGURE 3: Hypothetical mechanism for the observation that the phosphorylation of memapsin 2 cytosolic peptide enhances its binding to the VHS domain of GGAs. Memapsin 2 cytosolic octapeptide, which contains a VHS-recognition ACDL motif in the sequence of AD**D**IS**LL**K (essential residues in bold), prefers an extended conformation in solution (upper left). The charge distribution is optimal in such a conformation (acidic residues, white balls with black bar; basic residue, black ball with white cross; neutral residues, white balls). The phosphorylation of the serine residue (arrow 1) resulted in a different charge distribution (lower left) and assuming a new preferred conformation (reaction 2) where phosphoserine (S_P) is in an ionic interaction (dotted line) with the C-terminal lysine (upper right). Such a conformation places three essential residues (D, L, and L) on the same side of the peptide and thus facilitates its binding to VHS (arrow 3, lower right) by lowering the binding entropy.

Table 3: Change in Enthalpy (ΔH) and Entropy (ΔS) upon Binding of Phosphorylated and Nonphosphorylated Memapsin 2 Peptide to the VHS Domain of GGAs

peptide/VHS source	K_d (μM)	ΔH (kcal/mol)	ΔS (cal/mol)
M2-8/GGA1	399 ± 41	−15.7 ± 1.2	−36.6
M2-8(P)/GGA1	40 ± 5	−10.9 ± 1.3	−16.2
M2-8/GGA2	412 ± 52	−15.8 ± 1.2	−36.9
M2-8(P)/GGA2	101 ± 4	−16.1 ± 1.3	−35.2
M2-8/GGA3	307 ± 25	−12.5 ± 0.9	−25.3
M2-8(P)/GGA3	22 ± 3	−3.8 ± 0.1	8.8

binding to VHS. To test this hypothesis, we calculated the binding energies from the isothermal calorimetric studies of memapsin 2 native and phosphorylated peptides in Table 1. As shown in Table 3, the phosphorylation significantly reduced the entropy loss in both GGA1 (from −36.6 to −16 cal/mol, at 30 °C) and GGA3 (from −25 to +8.8 cal/mol, at 30 °C). The change of binding entropy due to phosphorylation is small in GGA2 (from −36.9 to −35.2 cal/mol, at 30 °C). This may be related to the unique conformational change of GGA2 VHS upon ligand binding (*27*), a phenomenon not seen for the VHS domains of GGA1 and GGA3, and could have reduced the entropic benefit of the phosphorylation. The conservation in the topology of the ACDL-binding residue among GGAs argues for the uniformity of this mechanism in the interaction of memapsin 2 and VHS domains. The charge distribution in the VHS domains may also contribute to the stability of the phosphoserine to lysine interaction in memapsin 2. In the crystal structure, the C-terminal lysine is located at the midway between VHS residues Lys^{101} and Lys^{141}. The salt linkage to phosphoserine and the conformation it adopted would relieve the C-terminal lysine from the charge repulsion of these two groups.

Of particular significance is the highest binding improvement of GGA3 VHS upon the phosphorylation of the memapsin 2 C-tail peptide. GGA3 is known to exist in two variants from differential splicing of its messenger RNA (*18*). The shorter form is missing part of the VHS domain and does not bind memapsin 2 peptides (data not shown). The longer form used in this study is predominantly expressed in the brain (*33*) where memapsin 2 is also expressed at a higher level than in most of the other organs (*1*). This correlation posts an intriguing possibility that the specificity of GGA function in memapsin 2 intracellular transport may be determined, in addition to the interaction studied here, by the tissue expression of GGAs.

ACKNOWLEDGMENT

The authors thank Dr. Jean Hartsuck for helpful discussion and critical reading of this manuscript, Marcus Dehdarani for technical assistance, Dr. K. Nakayama for the GGA1 vector, and Dr. M. S. Robinson for cDNA clones of GGA1 and GGA2. J.T. is holder of the J.G. Puterbaugh Chair in Biomedical Research at the Oklahoma Medical Research Foundation.

REFERENCES

1. Lin, X., Koelsch, G., Wu, S., Downs, D., Dashti, A., and Tang, J. (2000) Human aspartic protease memapsin 2 cleaves the β-amyloid precursor protein, *Proc. Natl. Acad. Sci. U.S.A. 97*, 1456−1460.
2. Vassar, R., Bennett, B. D., Babu-Khan, S., Mendiaz, E. A., Denis, P., Teplow, D. B., Ross, S., Amarante, P., Loeloff, R., Luo, Y., Fisher, S., Fuller, J., Edenson, S., Lile, J., Jarosinski, M. A., Biere, A. L., Curran, E., Burgess, T., Louis, J. C., Collins, F., Treanor, J., Rogers, G., and Citron, M. (1999) β-secretase cleavage of Alzheimer's amyloid precursor protein by the transmembrane aspartic protease BACE, *Science 286*, 735−741.
3. Hussain, J., Powell, D., Howlett, D. R., Tew, D. G., Meek, T. D., Chapman, C., Gloger, I. S., Murphy, K. E., Southan, C. D., Ryan, D. M., Smith, T. S., Simmons, D. L., Walsh, F. S., Dingwall, C., and Christie, G. (1999) Identification of a novel aspartic protease (Asp 2) as β-secretase, *Mol. Cell Neurosci. 14*, 419−427.
4. Yan, R., Bienkowski, M. J., Shuck, M. E., Miao, H., Tory, M. C., Pauley, A. M., Brashier, J. R., Stratman, N. C., Mathews, W. R., Buhl, A. E., Carter, D. B., Tomasselli, A. G., Parodi, L. A., Heinrikson, R. L., and Gurney, M. E. (1999) Membrane-anchored aspartyl protease with Alzheimer's disease β-secretase activity, *Nature 402*, 533−537.
5. Selkoe, D. (2001) Alzheimer's disease: genes, proteins, and therapy, *Physiol. Rev. 81*, 741−766.
6. Hong, L., Koelsch, G., Lin, X., Wus, S., Terzyan, S., Ghosh, A., Zhang, X. C., and Tang, J. (2000) Structure of the Protease Domain of Memapsin 2 (β-Secretase) Complex with Inhibitor, *Science 290*, 150−153.
7. Bennett, B. D., Denis, P., Haniu, R., Teplow, D. B., Kahn, S., Louis, J. C., Citron, M., and Vassar, R. (2000) A furin-like convertase mediates propeptide cleavage of BACE, the Alzheimer's β-secretase, *J. Biol. Chem. 275*, 37712−37717.
8. Creemers, J. W., Dominguez, D. I., Plets, E., Serneels, L., Taylor, N. A., Multharp, G., Craessaerts, K., Annaert, W., and De Strooper, B. (2000) Processing of β-secretase by furin and other members of the proprotein convertase family, *J. Biol. Chem. 276*, 4211−4217.
9. Capell, A., Steiner, H., Willem, M., Kaiser, H., Meyer, C., Walter, J., Lammich, S., Multhaup, G., and Haass, C. (2000) Maturation and pro-peptide cleavage of β-secretase, *J. Biol. Chem. 275*, 30849−30854.
10. Huse, J. T., Pijak, D. S., Leslie, G. J., Lee, V. M.-Y., and Doms, R. W. (2000) Maturation and endosomal targeting of β-site amyloid precursor protein-cleaving enzyme. The Alzheimer's disease β-secretase, *J. Biol. Chem. 275*, 33729−33737.

11. Ermolieff, J., Loy, J. A., Koelsch, G., and Tang, J. (2000) Proteolytic activation of recombinant pro-memapsin 2 (pro-β-secretase) studied with new fluorogenic substrates, *Biochemistry 39*, 12450−12456.
12. Walter, J., Fluhrer, R., Hartung, B., Willem, M., Kaether, C., Capell, A., Lammich, S., Multhaup, G., and Haass, C. (2001) Phosphorylation regulates intracellular trafficking of β-secretase, *J. Biol. Chem. 276*, 14634−14641.
13. Pastorino, L., Ikin, A. F., Nairn, A. C., Pursnani, A., and Buxbaum, J. D. (2002) The carboxyl-terminus of BACE contains a sorting signal that regulates BACE trafficking but not the formation of total Aβ, *Mol. Cell. Neurosci. 19*, 175−185.
14. He, X., Chang, W. P., Koelsch, G., and Tang, J. (2002) Memapsin 2 (β-secretase) cytosolic domain binds to the VHS domains of GGA1 and GGA2: implications on the endocytosis mechanism of memapsin 2, *FEBS Lett. 524*, 183−187.
15. Puertollano, R., Aguilar, R. C., Gorshkova, I., Crouch, R. J., and Bonifacino, J. S. (2001) Sorting of mannose 6-phosphate receptors mediated by the GGAs, *Science 292*, 1712−1716.
16. Zhu, Y., Doray, B., Poussu, A., Lehto, V. P., and Kornfeld, S. (2001) Binding of GGA2 to the lysosomal enzyme sorting motif of the mannose 6-phosphate receptor, *Science 292*, 1716−1718.
17. Taktsu, H., Katoh, Y., Shiba, Y., and Nakayama, K. (2001) Golgi-localizing, γ-adaptin ear homology domain, ADP-ribosylation factor-binding (GGA) proteins interact with acidic dileucine sequences within the cytoplasmic domains of sorting receptors through their Vps27p/Hrs/STAM (VHS) domains, *J. Biol. Chem. 276*, 28541−28545.
18. Nielsen, M. S., Madsen, P., Christensen, E. I., Nykjaer, A., Gliemann, J., Kasper, D., Pohlmann, R., and Petersen, C. M. (2001) The sortilin cytoplasmic tail conveys Golgi-endosome transport and binds the VHS domain of the GGA2 sorting protein, *EMBO J. 20*, 2180−2190.
19. Rosouius, O., Mieskes, G., Issinger, O. G., Korner, C., Schmidt, B., von Figura, K., and Braulke, T. (1993) Characterization of phosphorylation sites in the cytoplasmic domain of the 300 kDa mannose-6-phosphate receptor, *Biochem. J. 292*, 833−838.
20. Meresse, S., Ludwig, T., Frank, R., and Hoflack, B. (1990) Phosphorylation of the cytoplasmic domain of the bovine cation-independent mannose-6-phosphate receptor. Serines 2421 and 2492 are the targets of a casein kinase II associated to the Golgi-derived HAI adaptor complex, *J. Biol. Chem. 265*, 18833−18842.
21. Meresse, S., and Holflack, B. (1993) Phosphorylation of the cation-independent mannose-6-phosphate receptor is closely associated with its exit from the trans-Golgi network, *J. Cell Biol. 120*, 67−75.
22. Kato, Y., Misra, S., Puertollano, R., Hurley, J. H., and Bonifacino, J. S. (2002) Phosphoregulation of sorting signal−VHS domain interaction by a direct electrostatic mechanism, *Nat. Struct. Biol. 9*, 532−536.
23. Hirst, J., Lui, W. W., Bright, N. A., Totty, N., Seaman, M. N., and Robinson, M. S. (2000) A family of proteins with γ-adaptin and VHS domains that facilitate trafficking between the trans-Golgi network and the vacuole/lysosome, *J. Cell Biol. 149*, 67−80.
24. Mattera, R., Arighi, C. N., Lodge, R., Zerial, M., and Bonifacino, J. S. (2003) Divalent interaction of the GGAs with the rabaptin-5-rabex-5 complex, *EMBO J. 22*, 78−88.
25. Misra, S., Puertollano, R., Kato, Y., Bonifancino, J. S., and Hurley, J. H. (2002) Structural basis for acidic-cluster-dileucine sorting-signal recognition by VHS domains, *Nature 415*, 933−937.
26. Shiba, T., Takatsu, H., Nogi, T., Matsugaki, N., Kawasaki, M., Igarashi, N., Suzuki, M., Kato, R., Earnest, T., Nakayama, K., and Wakatsuki, S. (2002) Structural basis for recognition of acidic-cluster dileucine sequence by GGA1, *Nature 415*, 937−941.
27. Zhu, G., He, X., Zhai, P., Terzyan, S., Tang, J., and Zhang, X. C. (2003) Crystal structure of GGA2 VHS domain and its implication in plasticity in the ligand binding pocket, *FEBS Lett. 537*, 171−176.
28. Otwinowski, Z., and Minor, W. (1997) Processing of X-ray diffraction data collected in oscillation mode, *Methods Enzymol. 276*, 307−326.
29. Matthews, B. W. (1968) Solvent contents of protein crystals, *J. Mol. Biol. 33*, 491−497.
30. Navaza, J. (1994) AMoRe; an automated package for molecular replacement, *Acta Crystallogr., Sect. A: Found. Crystallogr. 50*, 157−163.
31. Roussel, A., and Cambillau, C. (1989) *Silicon Graphics Geometry Partners Directory*, pp 77−79, Silicon Graphics, Mountain View, CA.
32. Brunger, A. T., Adams, P. D., Clore, G. M., DeLano, W. L., Gros, P., Grosse-Kunstleve, R. W., Jiang, J. S., Kuszewski, J., Nilges, M., Pannu, N. S., Read, R. J., Rice, L. M., Simonson, T., and Warren, G. L. (1998) Crystallography & NMR system: A new software suite for macromolecular structure determination, *Acta Crystallogr. D Biol. Crystallogr. 54*, 905−921.
33. Wakasugi, M., Waguri, S., Kametaka, S., Tomiyama, Y., Kanamori, S., Shiba, Y., Nakayama, K., and Uchiyama, Y. (2003) Predominant expression of the short form of GGA3 in human cell lines and tissues, *Biochem. Biophys. Res. Commun. 306*, 687−692.

BI035199H